



Synthesis, optophysical and electrochemical properties of bipolar-transporting europium(III) complexes with carbazole and oxadiazole units

Liang Li, Yu Liu^{*}, Haipeng Guo, Yafei Wang, Yunbo Cao, Aihui Liang, Hua Tan, Hongrui Qi, Meixiang Zhu, Weiguo Zhu^{*}

College of Chemistry, Key Lab of Environment-Friendly Chemistry and Application in Ministry of Education, Xiangtan University, Xiangtan 411105, China

ARTICLE INFO

Article history:

Received 20 April 2010

Received in revised form 11 June 2010

Accepted 2 July 2010

Available online 15 July 2010

Keywords:

Europium(III) complexes

Synthesis

Optophysical properties

Bipolar-transporting

Carbazole

1,3,4-Oxadiazole

ABSTRACT

A series of bipolar-transporting europium(III) complexes containing carbazole and oxadiazole units were synthesized and characterized. Two intense UV absorption bands at around 286 nm and 352 nm, and sharply red emissions peaked at 614 nm were observed for these europium complexes in dichloromethane. Importantly, the bipolar-transporting europium(III) complexes exhibited higher thermal stability, more intense UV absorption at 286 nm and twofold increased photoluminescent quantum yield compared to the reported red chromophore of tri(dibenzoylmethane) (1,10-phenanthroline) europium(III).

© 2010 Elsevier Ltd. All rights reserved.

1. Introduction

Europium complexes have attracted a great deal of attention in recent decades because of their highly monochromatic red emission from f-orbit electron transition of europium(III) ion and 100% theoretical emission quantum efficiency resulting from both singlet and triplet excitonic emission in organic and polymeric light-emitting devices (OLEDs and PLEDs).^{1–6} The best europium complex-doped OLED was developed by Kido group, which consisted of tri(dibenzoylmethane) (4,7-biphenyl-1,10-phenanthroline) europium(III) dopant and presented an external quantum efficiency (EQE) as high as 7.5% at 0.02 mA/cm² with corresponding luminous efficiency of 10 lm/W, as well as gave the maximum brightness of 2797 cd/m².⁷ The high-efficiency europium complex-doped PLEDs with an EQE of about 1.0% were demonstrated by McGehee and our groups, respectively.^{8,9} These performances of the europium complex-doped devices have not met practical requirement yet.

Low EQE and brightness for the europium complex-doped devices were mainly attributed to the poor carrier-transporting ability of europium complexes.¹⁰ Therefore, two main approaches have been developed to improve properties of the europium complex-

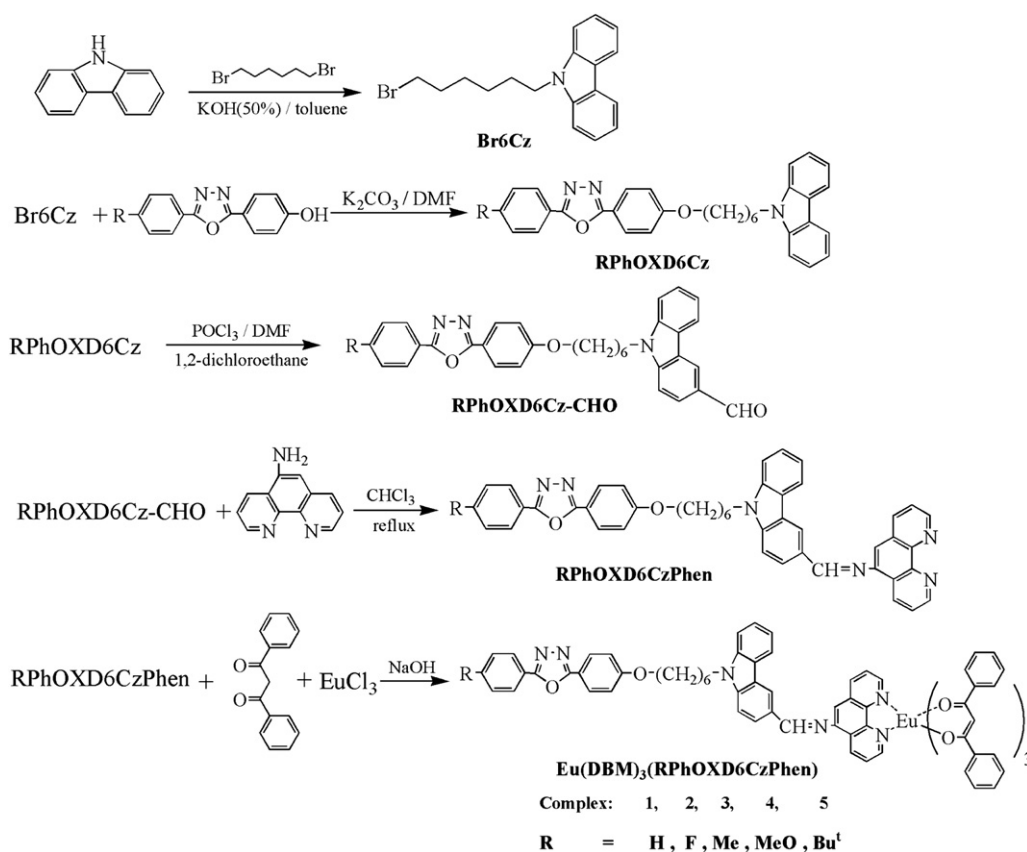
doped devices. The first approach is doping europium complexes into polymers or small molecular compounds with high hole- and/or electron mobility. The second approach is grafting hole- or electron-transporting units on anionic or ancillary ligands.^{11–14} The grafted hole- and electron-transporting groups (i.e., carrier-transporting groups) mainly contain carbazole,^{11–13} triphenylamine,¹⁴ and oxadiazole groups.^{15,16} Most of europium(III) complexes were tuned by grafting one of two carrier-transporting units in the same ligand. Recently, the first example of modification of europium complex has been reported by Zhang group, in which both hole- and electron-transporting units were, respectively, attached on diketone and phenanthroline.¹⁷ This europium(III) complex involving both hole- and electron-transporting functional groups exhibited a significantly improved device performance with a high brightness of 1845 cd/m² and current efficiency of 2.62 cd/A, as well as a low turn-on voltage of 5.5 V. It shows that incorporating both hole- and electron-transporting units into europium complexes is available for improving electroluminescent properties of europium complexes.

A promising europium complex used as a red-emitting electroluminescent material should have excellent optophysical and electrochemical properties at least. In order to further study the influence of bipolar-transporting units on these properties, we designed and synthesized another class of novel bipolar-transporting europium complexes by incorporating both hole-transporting carbazole and electron-transporting oxadiazole units into

^{*} Corresponding authors. Tel.: +86 731 58298280; fax: +86 731 58292251; e-mail addresses: liuyu03b@126.com (Y. Liu), zhuwg18@126.com (W. Zhu).

phenanthroline ligand. The structure of europium(III) complexes and their synthetic route are shown in Scheme 1. As dibenzoylmethane (HDBM) has relatively high PL efficiency and the bipolar-transporting units have been confirmed to have an ability to improve optoelectronic property in OLEDs,¹⁸ this class of europium(III) complexes is expected to exhibit improved photophysical properties. In research on thermal stability, photophysical, and electrochemical properties of these europium complexes, we found that this kind of europium complexes with both carbazole and oxadiazole units presented higher thermal stability, more intense UV absorption at high-energy area and higher emission quantum efficiency compared to the reported tri(dibenzoylmethane) (1,10-phenanthroline) europium(III) [Eu(DBM)₃Phen].

a heating rate of 20 °C/min using a Perkin–Elmer TGA-7 thermal analyzer. The FT-IR spectra were obtained on a Perkin–Elmer spectrum one Fourier transform infrared spectrometer (KBr pellet). Ultraviolet-visible (UV–vis) spectra were measured with a Lambda 25 spectrophotometer. Photoluminescence spectra were conducted on a Perkin–Elmer LS55 luminescence spectrometer with a xenon lamp as a light source. Cyclic voltammetry was carried out on a CHI660A electrochemical work station in a solution of tetrabutylammonium hexafluorophosphate (Bu₄NPF₆) (0.1 M) and acetonitrile at a scan rate of 50 mV/s and room temperature under nitrogen flow protection. These europium complexes were dissolved in the above solution (1 mg cm^{−3}). A platinum electrode was used as the working electrode. A platinum wire was used as the



Scheme 1. Synthetic route of the bipolar-transporting europium complexes.

2. Experimental

2.1. General

Carbazole, 1,6-dibromohexane, dibenzoylmethane (HDBM), tetrahydrofuran (THF), *N,N*-dimethylformamide (DMF), dichloromethane (DCM), ethanol, Eu₂O₃ (99.5%), K₂CO₃ and KOH were analytical reagents and purchased from some reagent plants in China. 4-(5-Aryl-1,3,4-oxadiazol-2-yl)phenol derivatives were prepared according to previous report.^{19,20} 5-Amino-1,10-phenanthroline was prepared according to the literature procedure.²¹ All other reagents were used from commercial sources, unless otherwise stated.

All ¹H NMR spectra were acquired at a Bruker Dex-400NMR instrument using CDCl₃ as solvent. Elemental analysis was carried out on a Heraeus CHN-Rapid elemental analyzer. Thermogravimetric analysis (TGA) was performed under a nitrogen atmosphere at

counter electrode and a calomel electrode was used as the reference electrode. Ferrocene was employed as the reference of redox system.

2.2. Synthesis of 9-(6-bromohexyl)carbazole (1)

50 mL of 50% KOH aqueous solution was added to a solution of 12.0 g (41.1 mmol) carbazole, 9.6 mL (61.5 mmol) 1,6-dibromohexane, a catalytic amount of tetrabutylammonium bromide, and 50 mL toluene under stirring in a 250 mL three-necked flask and was refluxed for 24 h. The mixture was then evaporated to remove the solvent under vacuum. The residue was extracted with DCM (3×20 mL). The organic layer was washed with water, dried over anhydrous MgSO₄, and then filtered. The filtrate was evaporated and the residue was purified by silica gel column chromatography using hexanes/DCM (v/v=4: 1) as eluent to provide 9.2 g white solid with a yield of 66.8%. Mp: 70–72 °C. ¹H NMR (400 MHz,

CDCl_3): δ ppm 8.09–8.11 (d, $J=8.4$ Hz, 2H), 7.39–7.48 (m, 4H), 7.21–7.25 (t, 2H), 4.30–4.33 (t, 2H), 3.34–3.37 (t, 2H), 1.79–1.92 (m, 4H), 1.44–1.53 (m, 4H).

2.3. Synthesis of 9-(6-(4-(5-phenyl-1,3,4-oxadiazol-2-yl)phenoxy)hexyl)-9H-carbazole (HPhOXD6Cz)

9-(6-Bromohexyl)carbazole 3.4 g (8.0 mmol) was added to a mixture of 2.4 g (10.0 mmol) 2-(4-hydroxyphenyl)-5-phenyl-1,3,4-oxadiazol (HPhOXDOH), 4.4 g (30.0 mmol) dispersing K_2CO_3 , 35.0 mL DMF and 0.1 g KI under stirring for 30 min at room temperature. The mixture was refluxed for 24 h under nitrogen atmosphere and allowed to cool to room temperature. Then the reaction mixture was subsequently poured into ice water (100 mL) and extracted with DCM (3×30 mL). The organic layer was washed with water, dried over anhydrous MgSO_4 , and then filtered. The filtrate was evaporated and the residue was purified by recrystallization using THF and ethanol ($v/v=1:2$) as solvent to provide 1.7 g pale yellow solid with a yield of 50.8%. Mp: 120–122 °C. ^1H NMR (400 MHz, CDCl_3): δ ppm 8.14–8.10 (m, 4H), 8.07–8.04 (d, $J=9.2$ Hz, 2H), 7.54–7.41 (m, 7H), 7.22–7.24 (d, $J=8.4$ Hz, 2H), 6.98–6.96 (d, $J=8.4$ Hz, 2H), 4.36–4.33 (t, 2H), 4.00–3.96 (t, 2H), 1.97–1.72 (m, 4H), 1.53–1.47 (m, 4H).

2.4. Synthesis of 9-(6-(4-(5-(4-fluorophenyl)-1,3,4-oxadiazol-2-yl)phenoxy)hexyl)-9H-carbazole (FPhOXD6Cz)

FPhOXD6Cz was synthesized according to the method described in Section 2.3. A pale yellow solid was obtained with a yield of 56.8%. Mp: 125–126 °C. ^1H NMR (400 MHz, CDCl_3): δ ppm 8.13–8.10 (m, 4H), 8.05–8.03 (d, $J=8.6$ Hz, 2H), 7.47–7.43 (m, 4H), 7.25–7.22 (m, 4H), 6.98–6.96 (d, $J=8.4$ Hz, 2H), 4.37–4.33 (t, 2H), 4.00–3.97 (t, 2H), 1.96–1.93 (t, 2H), 1.81–1.77 (t, 2H), 1.53–1.47 (m, 4H).

2.5. Synthesis of 9-(6-(4-(5-*p*-tolyl-1,3,4-oxadiazol-2-yl)phenoxy)hexyl)-9H-carbazole (MePhOXD6Cz)

MePhOXD6Cz was synthesized according to the method described in Section 2.3. A pale yellow solid was obtained with a yield of 50.8%. Mp: 122–123 °C. ^1H NMR (400 MHz, CDCl_3): δ ppm 8.12–8.02 (m, 6H), 7.47–7.41 (m, 4H), 7.26–7.23 (d, $J=9.4$ Hz, 2H), 7.04–6.95 (m, 4H), 4.59–4.33 (t, 2H), 4.00–3.96 (t, 2H), 2.44 (s, 3H), 1.98–1.75 (m, 4H), 1.58–1.47 (m, 4H).

2.6. Synthesis of 9-(6-(4-(5-(4-methoxyphenyl)-1,3,4-oxadiazol-2-yl)phenoxy)hexyl)-9H-carbazole (MeOPhOXD6Cz)

MeOPhOXD6Cz was synthesized according to the method described in Section 2.3. A white solid was obtained with a yield of 49.2%. Mp: 123–125 °C. ^1H NMR (400 MHz, CDCl_3): δ ppm 8.12–8.02 (m, 6H), 7.47–7.41 (m, 4H), 7.26–7.23 (d, $J=9.4$ Hz, 2H), 7.04–6.95 (m, 4H), 4.36–4.33 (t, 2H), 4.00–3.96 (t, 2H), 3.89 (s, 3H), 1.98–1.75 (m, 4H), 1.58–1.47 (m, 4H).

2.7. Synthesis of 9-(6-(4-(5-(4-*tert*-butylphenyl)-1,3,4-oxadiazol-2-yl)phenoxy)hexyl)-9H-carbazole (Bu^tPhOXD6Cz)

Bu^tPhOXD6Cz was synthesized according to the method described in Section 2.3. A pale yellow solid was obtained with a yield of 54.0%. Mp: 118–119 °C. ^1H NMR (400 MHz, CDCl_3): δ ppm 8.12–8.10 (d, $J=8.4$ Hz, 2H), 8.05–8.03 (m, 4H), 7.55–7.53 (d, $J=8.4$ Hz, 2H), 7.46–7.40 (m, 4H), 7.23–7.25 (d, $J=8.4$ Hz, 2H), 6.97–6.95 (d, $J=8.5$ Hz, 2H), 4.36–4.33 (t, 2H), 4.00–3.96 (t, 2H), 1.98–1.75 (m, 4H), 1.58–1.48 (m, 4H), 1.37 (s, 9H).

2.8. Synthesis of 9-(6-(4-(5-phenyl-1,3,4-oxadiazol-2-yl)phenoxy)hexyl)-9H-carbazole-3-carbaldehyde (HPhOXD6Cz-CHO)

Phosphorus oxychloride 2.85 mL (30.5 mmol) was added dropwise into a solution of 1.02 mL (45.8 mmol) DMF and 30 mL 1,2-dichloroethane with stirring under ice bath and nitrogen atmosphere. The mixture was stirred for another 1 h at room temperature, and 1.7 g (4.03 mmol) HPhOXD6Cz dissolved in DMF (10 mL) was added into it. Then the reaction temperature was raised to 85 °C and the mixture was continued to be stirred for 24 h. The resulting mixture was permitted to cool to room temperature and poured into ice water (50 mL), then extracted with DCM (3×30 mL). The resulting organic layer was washed with water, dried over anhydrous MgSO_4 , and filtered. The filtrate was evaporated and the residue was purified by silica gel column chromatography using hexanes/ethyl acetate ($v/v=3:1$) as eluent to provide 0.94 g yellow solid with a yield of 60.2%. Mp: 100–100.5 °C. ^1H NMR (400 MHz, CDCl_3): δ ppm 10.11 (s, 1H), 8.63 (s, 1H), 8.19–8.02 (m, 6H), 7.55–7.47 (m, 6H), 6.99–6.97 (d, $J=8.8$ Hz, 2H), 4.41–4.37 (t, 2H), 4.02–3.98 (t, 2H), 2.01–1.93 (m, 2H), 1.82–1.78 (m, 2H), 1.56–1.49 (m, 4H).

2.9. Synthesis of 9-(6-(4-(5-(4-fluorophenyl)-1,3,4-oxadiazol-2-yl)phenoxy)hexyl)-9H-carbazole-2-carbaldehyde (FPhOXD6Cz-CHO)

FPhOXD6Cz-CHO was synthesized according to the method described in Section 2.8. A yellow solid was obtained with a yield of 51.2%. Mp: 98–99 °C. ^1H NMR (400 MHz, CDCl_3): δ ppm 10.11 (s, 1H), 8.64 (s, 1H), 8.19–8.02 (m, 6H), 7.55–7.47 (m, 6H), 6.99–6.97 (d, $J=8.8$ Hz, 2H), 4.42–4.38 (t, 2H), 4.02–3.99 (t, 2H), 2.00–1.79 (m, 4H), 1.56–1.49 (m, 4H).

2.10. Synthesis of 9-(6-(4-(5-*p*-tolyl-1,3,4-oxadiazol-2-yl)phenoxy)hexyl)-9H-carbazole-2-carbaldehyde (MePhOXD6Cz-CHO)

MePhOXD6Cz-CHO was synthesized according to the method described in Section 2.8. A yellow solid was obtained with a yield of 49.2%. Mp: 99–100 °C. ^1H NMR (400 MHz, CDCl_3): δ ppm 10.11 (s, 1H), 8.63 (s, 1H), 8.19–8.01 (m, 6H), 7.57–7.47 (m, 3H), 7.34–7.33 (d, $J=7.9$ Hz, 3H), 6.98–6.96 (d, $J=8.6$ Hz, 2H), 4.40–4.14 (t, 2H), 4.08–3.80 (t, 2H), 2.45 (s, 3H), 2.09–1.80 (m, 4H), 1.58–1.37 (m, 4H).

2.11. Synthesis of 9-(6-(4-(5-(4-methoxyphenyl)-1,3,4-oxadiazol-2-yl)phenoxy)hexyl)-9H-carbazole-2-carbaldehyde (MeOPhOXD6Cz-CHO)

MeOPhOXD6Cz-CHO was synthesized according to the method described in Section 2.7. A yellow solid was obtained with a yield of 51.2%. Mp: 99–101 °C. ^1H NMR (400 MHz, CDCl_3): δ ppm 10.11 (s, 1H), 8.64 (s, 1H), 8.19–8.02 (m, 6H), 7.55–7.47 (m, 4H), 7.06–7.04 (d, $J=8.6$ Hz, 2H), 6.98–6.96 (d, $J=8.6$ Hz, 2H), 4.41–4.38 (t, 2H), 4.02–3.98 (t, 2H), 3.91 (s, 3H), 2.01–1.96 (m, 2H), 1.82–1.75 (m, 4H), 1.56–1.49 (m, 4H).

2.12. Synthesis of 9-(6-(4-(5-(4-*tert*-butylphenyl)-1,3,4-oxadiazol-2-yl)phenoxy)hexyl)-9H-carbazole-2-carbaldehyde (Bu^tPhOXD6Cz-CHO)

Bu^tPhOXD6Cz-CHO was synthesized according to the method described in Section 2.8. A yellow solid was obtained with a yield of 57.2%. Mp: 97–99 °C. ^1H NMR (400 MHz, CDCl_3): δ ppm 10.10 (s, 1H), 8.62 (s, 1H), 8.18–8.00 (m, 6H), 7.55–7.46 (m, 6H), 6.97–6.95

(d, $J=8.7$ Hz, 2H), 4.40–4.36 (t, 2H), 4.00–3.97 (t, 2H), 2.04–1.75 (m, 4H), 1.56–1.49 (m, 4H), 1.37 (s, 9H).

2.13. Synthesis of *N*-((9-((4-(5-phenyl-1,3,4-oxadiazol-2-yl)phenoxy)methyl)-9*H*-carbazol-3-yl)methylene)-1,10-phenanthroline-5-amine (HPhOXD6CzPhen)

A mixture of 0.1 g (1.05 mmol) 5-amino-1,10-phenanthroline, 0.5 g (1.2 mmol) HPhOXD6Cz-CHO, 15 mL CHCl_3 , and a catalytic amount of acetic acid was refluxed for 6 h. After evaporated solvent, a yellow solid was formed. The solid crude was collected and washed with methanol, and then was purified by recrystallization from ethanol to provide 0.32 g yellow solid with a yield of 70%. Mp: 81–82 °C. ^1H NMR (400 MHz, CDCl_3): δ ppm 9.24–9.22 (d, $J=8.4$ Hz, 1H), 9.13–9.12 (d, $J=8.4$ Hz, 1H), 8.87–8.75 (t, 2H), 8.23–8.20 (m, 2H), 8.06–8.01 (q, 5H), 7.36–7.26 (m, 8H), 6.98–6.96 (d, $J=8.6$ Hz, 2H), 4.44–4.40 (t, 2H), 4.01–3.98 (t, 2H), 1.99–1.97 (m, 4H), 1.83–1.80 (m, 4H).

2.14. Synthesis of *N*-((9-((4-(5(4-fluorophenyl)-1,3,4-oxadiazol-2-yl)phenoxy)methyl)-9*H*-carbazole-3-yl)methylene)-1,10-phenanthroline-5-amine (FPhOXD6CzPhen)

FPhOXD6CzPhen was synthesized according to the method described in Section 2.13. A yellow solid was obtained with a yield of 62%. Mp: 82–83 °C. ^1H NMR (400 MHz, CDCl_3): δ ppm 9.24–9.23 (d, $J=5.4$ Hz, 1H), 9.13–9.12 (d, $J=5.4$ Hz, 1H), 8.85–8.75 (t, 2H), 8.23–8.20 (m, 2H), 8.06–8.03 (q, 5H), 7.36–7.26 (m, 8H), 6.98–6.96 (d, $J=8.4$ Hz, 2H), 4.44–4.41 (t, 2H), 4.02–3.99 (t, 2H), 2.06–1.98 (d, $J=8.6$ Hz, 4H), 1.82–1.79 (t, 4H).

2.15. Synthesis of *N*-((9-((4-(5-*p*-tolyl-1,3,4-oxadiazol-2-yl)phenoxy)methyl)-9*H*-carbazol-3-yl)methylene)-1,10-phenanthroline-5-amine (MePhOXD6CzPhen)

MePhOXD6CzPhen was synthesized according to the method described in Section 2.12. A yellow solid was obtained with a yield of 68%. Mp: 82–83 °C. ^1H NMR (400 MHz, CDCl_3): δ ppm 9.24–9.23 (d, $J=5.4$ Hz, 1H), 9.13–9.12 (d, $J=6.4$ Hz, 1H), 8.87–8.75 (t, 2H), 8.23–8.20 (m, 2H), 8.06–8.01 (q, 5H), 7.36–7.26 (m, 8H), 6.98–6.96 (d, $J=8.4$ Hz, 2H), 4.44–4.40 (t, 2H), 4.01 (s, 2H), 2.45 (s, 3H), 2.00–1.70 (m, 8H).

2.16. Synthesis of *N*-((9-((4-(5(4-methoxyphenyl)-1,3,4-oxadiazol-2-yl)phenoxy)methyl)-9*H*-carbazol-3-yl)methylene)-1,10-phenanthroline-5-amine (MeOPhOXD6CzPhen)

MeOPhOXD6CzPhen was synthesized according to the method described in Section 2.13. A yellow solid was obtained with a yield of 50%. Mp: 84–85 °C. ^1H NMR (400 MHz, CDCl_3): δ ppm 9.36–9.35 (d, $J=5.4$ Hz, 1H), 9.13–9.12 (d, $J=6.4$ Hz, 1H), 8.85–8.75 (t, 2H), 8.23–8.20 (m, 2H), 8.06–8.01 (q, 5H), 7.36–7.26 (m, 8H), 7.00–6.96 (m, 2H), 4.41–4.38 (t, 2H), 4.01–3.98 (t, 2H), 3.90 (s, 3H), 1.99–1.79 (m, 8H).

2.17. Synthesis of *N*-((9-((4-(5-(4-*tert*-butylphenyl)-1,3,4-oxadiazol-2-yl)phenoxy)methyl)-9*H*-carbazol-3-yl)methylene)-1,10-phenanthroline-5-amine (Bu^tPhOXD6CzPhen)

Bu^tPhOXD6CzPhen was synthesized according to the method described in Section 2.13. A yellow solid was obtained with a yield of 74.6%. Mp: 79–81 °C. ^1H NMR (400 MHz, CDCl_3): δ ppm 9.24–9.23 (d, $J=5.2$ Hz, 1H), 9.13–9.12 (d, $J=5.6$ Hz, 1H), 8.87–8.75 (t, 2H), 8.23–8.20 (m, 2H), 8.06–8.01 (q, 5H), 7.36–7.26 (m, 8H),

6.98–6.96 (d, $J=8.4$ Hz, 2H), 4.44–4.40 (t, 2H), 4.01–3.98 (t, 2H), 2.00–1.98 (d, $J=8.7$ Hz, 2H), 1.82–1.80 (t, 2H), 1.59–1.52 (m, 13H).

2.18. Synthesis of Eu(DBM)₃(HPhOXD6CzPhen)

Eu_2O_3 0.036 g (0.1 mmol) was dissolved in 1 mL concentrated hydrochloric acid was heated to 70–80 °C to form white $\text{EuCl}_3 \cdot 6\text{H}_2\text{O}$. This europium chloride was dissolved in ethanol (2.0 mL) for the following procedure. Then, a solution of 0.136 g (0.6 mmol) HDBM in 5 mL ethanol was added to a 25 mL three-necked flask and neutralized to pH=6 with 1 mol/L NaOH aqueous solution under stirring. The above europium chloride solution was then added dropwise into the HDBM solution with stirring. The reaction mixture was stirred for 30 min in room temperature and a solution of 0.150 g (0.2 mmol) HPhOXD6Cz-Phen in 2 mL THF was added to it. The mixture was then carefully adjusted to pH=6.5–7 again and continued to be stirred for 5 h at 50 °C. The resulting mixture was allowed to cool to room temperature and then added dropwise into 20 mL ethanol. The precipitate was formed and washed with water and ethanol alternately, further was purified by recrystallization with mixing solvents (THF and ethanol, v/v=1: 5) to provide 0.16 g yellow solid with a yield of 60.0%. Mp: 118–119 °C. FT-IR (KBr, cm^{-1}) 2923, 1610, 1594, 1549, 1517, 1496, 1477, 1458, 1411, 1308, 1219, 1175, 1067, 1024, 837, 808, 738, 723, 690, 520. Anal. Calcd for $\text{EuC}_{90}\text{H}_{69}\text{N}_6\text{O}_8$ (1514.96): C, 71.37; H, 4.59; N, 5.55. Found: C, 70.62; H, 5.04; N, 5.38.

2.19. Synthesis of Eu(DBM)₃(FPhOXD6CzPhen)

$\text{Eu}(\text{DBM})_3(\text{FPhOXD6CzPhen})$ was synthesized according to the method described in Section 2.19. A yellow solid was obtained with a yield of 58.0%. Mp: 118–120 °C. FT-IR (KBr, cm^{-1}) 2924, 1610, 1595, 1550, 1518, 1490, 1477, 1458, 1412, 1384, 1308, 1179, 1069, 841, 744, 737, 518. Anal. Calcd for $\text{EuC}_{90}\text{H}_{68}\text{FN}_6\text{O}_8$ (1532.5) C, 70.54; H, 4.47; N, 5.48. Found: C, 69.92; H, 4.34; N, 5.35.

2.20. Synthesis of Eu(DBM)₃(MePhOXD6CzPhen)

$\text{Eu}(\text{DBM})_3(\text{MePhOXD6CzPhen})$ was synthesized according to the method described in Section 2.18. A yellow solid was obtained with a yield of 65.0%. Mp: 117–117.5 °C. FT-IR (KBr, cm^{-1}) 2921, 1610, 1594, 1549, 1517, 1490, 1477, 1457, 1410, 1383, 1308, 1219, 1174, 1067, 814, 737, 722, 519. Anal. Calcd for $\text{EuC}_{91}\text{H}_{71}\text{N}_6\text{O}_8$ (1528.54) C, 71.50; H, 4.68; N, 5.50. Found: C, 70.60; H, 4.34; N, 5.41.

2.21. Synthesis of Eu(DBM)₃(MeOPhOXD6CzPhen)

$\text{Eu}(\text{DBM})_3(\text{MeOPhOXD6CzPhen})$ was synthesized according to the method described in Section 2.19. A yellow solid was obtained with a yield of 71.0%. Mp: 121–123 °C. FT-IR (KBr, cm^{-1}) 2937, 1611, 1594, 1549, 1517, 1496, 1477, 1458, 1411, 1384, 1219, 1175, 1067, 1024, 835, 807, 723, 608, 515. Anal. Calcd for $\text{EuC}_{91}\text{H}_{71}\text{N}_6\text{O}_9$ (1544.54): C, 70.76; H, 4.63; N, 5.44. Found: C, 73.52; H, 4.71; N, 4.45.

2.22. Synthesis of Eu(DBM)₃(Bu^tPhOXD6CzPhen)

$\text{Eu}(\text{DBM})_3(\text{Bu}^t\text{PhOXD6CzPhen})$ was synthesized according to the method described in Section 2.18. A yellow solid was obtained with a yield of 57.0%. Mp: 117–118 °C. FT-IR (KBr, cm^{-1}) 2930, 1610, 1594, 1549, 1517, 1496, 1477, 1458, 1411, 1384, 1219, 1175, 1067, 1023, 840, 808, 737, 721, 520. Anal. Calcd for $\text{EuC}_{94}\text{H}_{77}\text{N}_6\text{O}_8$ (1570.62): C, 71.88; H, 4.94; N, 5.35. Found: C, 71.62; H, 5.34; N, 5.39.

3. Results and discussion

3.1. IR absorption spectrum

These bipolar-transporting europium complexes displayed similar IR spectra. The stretching vibration peaks from the C=O, C=C, and C=N double bands were observed at 1594 cm^{-1} , 1517 cm^{-1} , and 1549 cm^{-1} , respectively. It indicates that β -diketone ligand of HDBM is coordinated to Eu^{3+} ion. The skeleton vibration from phenanthroline ring was found at 1538 cm^{-1} . Two C–H bending vibration peaks from phenanthroline ring were displayed at 812 cm^{-1} and 722 cm^{-1} . Another bending vibration peak from Eu–N was also observed at 519 cm^{-1} , which means that the phenanthroline derivatives of RPhOXD6CzPhen are also coordinated to Eu^{3+} ion.²² Therefore, the $\text{Eu}(\text{DBM})_3$ (RPhOXD6CzPhen) complexes were confirmed to be formed by IR data.

3.2. Thermal stability

The thermal properties of europium complexes were determined by TGA and the resulting TGA curves are shown in Figure S1. All the bipolar-transporting europium complexes presented an onset degradation temperature (T_d) for 5% weight loss as high as 300 $^{\circ}\text{C}$. For comparison, the T_d data are listed in Table 1. Obviously, these bipolar-transporting europium complexes exhibited better thermal stability than the known $\text{Eu}(\text{DBM})_3\text{Phen}$ complex. This implies that incorporating both carbazole and oxadiazole units into the phenanthroline ligand is favorable to enhance the thermal stability of their corresponding europium complexes. Furthermore, the substituent groups in oxadiazole units had a different effect on their thermal stability. Incorporating electron donor substituent group into oxadiazole unit is more available for the enhancement of thermal stability of the europium complexes.

Table 1

Thermal stability, optophysical and electrochemical properties of europium complexes

Complexes	UV–vis absorption ^a λ/nm [$\epsilon_{\text{max}}/\text{dm}^3 \text{mol}^{-1} \text{cm}^{-1}$]	λ_{em} ^b [nm]	T_d [$^{\circ}\text{C}$]	E_{ox} ^c [V]	E_{red} ^d [V]	E_{HOMO} ^e [eV]	E_{LUMO} ^f [eV]	E_g ^c [eV]
$\text{Eu}(\text{DBM})_3\text{Phen}$	352(29,945)	614	297	1.25	−1.96	−5.63	−2.42	3.21
Complex-1	292(32,274), 344(17,824)	433, 614	375	1.25	−1.80	−5.63	−2.58	3.05
Complex-2	286(52,479), 352(65,845)	403, 614	312	1.35	−1.70	−5.73	−2.68	3.05
Complex-3	286(38,540), 352(22,234)	429, 614	375	1.28	−1.84	−5.66	−2.54	3.12
Complex-4	286(49,564), 352(43,799)	407, 614	375	1.26	−1.94	−5.64	−2.44	3.20
Complex-5	286(65,423), 352(66,788)	419, 614	376	1.51	−1.53	−5.91	−2.87	3.04

^a Measured in CH_2Cl_2 at a concentration of 10^{-5} mol/L at 298 K.

^b Measured in CH_2Cl_2 at 298 K.

^c Estimated according to the reduction potential and the UV–vis absorption spectrum.

^d Calculated using equation: $E_{\text{red}} = (E_{\text{pa}} + E_{\text{pc}})/2$.

^e $E_{\text{HOMO}} = -(4.38 + E_{1/2}^{\text{ox}}) \text{ eV}$.

^f $E_{\text{LUMO}} = -(4.38 + E_{1/2}^{\text{red}}) \text{ eV}$.

3.3. UV absorption property

The normalized UV absorption spectra of europium complexes in DCM are illustrated in Figure 1. All the bipolar-transporting europium complexes showed an intense high-energy absorption band at about 288 nm and a strong low-energy absorption band at about 352 nm, in which the high-energy absorption band is attributed to $\pi-\pi^*$ transition of the bipolar-transporting phenanthroline ancillary ligand and low-energy absorption band is attributed to the singlet-singlet $\pi-\pi^*$ transition of the β -diketone ligand.²³ Compared to $\text{Eu}(\text{DBM})_3\text{Phen}$, the bipolar-transporting europium complexes of $\text{Eu}(\text{DBM})_3(\text{RPhOXD6CzPhen})$ exhibit similar low-energy absorption band, but red-shifted high-energy absorption band. This indicates that these bipolar-transporting units have a significant effect on UV absorption spectra of their europium complexes.

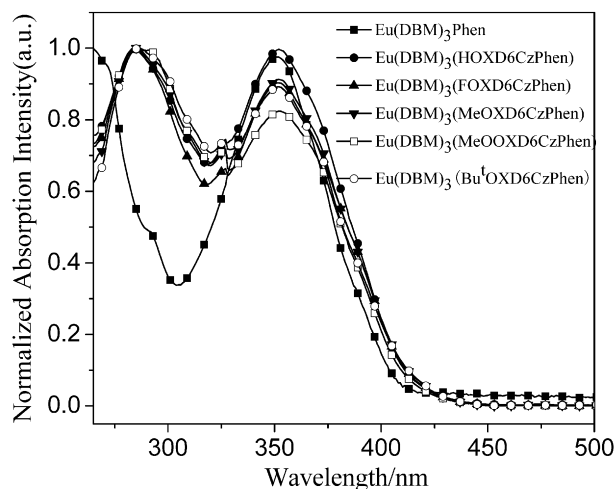


Figure 1. UV–vis absorption spectra of europium complexes in DCM.

3.4. Photoluminescence property

The normalized photoluminescence spectra of europium complexes in DCM and neat film at room temperature are shown in Figure 2a and Figure 2b, respectively. All these bipolar-transporting europium complexes displayed an intense sharp low-energy emission peak at 614 nm and a broad weak high-energy emission band between 350 and 550 nm, in which the low-energy emission peak is corresponding to $^5\text{D}_0 \rightarrow ^7\text{F}_2$ transition of $\text{Eu}(\text{III})$ ion, and the high-energy emission band is related to excited states of the phenanthroline derivatives of RPhOXD6CzPhen or to the ligand-to-metal charge transfer (LMCT) transitions resulting from the interaction between

the central Eu^{3+} ion and the ligand's first coordination shell.^{24,25} While the substituent group is butyl, the $\text{Eu}(\text{DBM})_3(\text{BuPhOXD6CzPhen})$ complex exhibited maximum high-energy emission band in DCM and neat film. In contrast, while the substituent group is fluorine, the $\text{Eu}(\text{DBM})_3(\text{FPhOXD6CzPhen})$ complex exhibit the minimum high-energy emission band in DCM and neat film. Compared to $\text{Eu}(\text{DBM})_3\text{Phen}$, $\text{Eu}(\text{DBM})_3(\text{FPhOXD6CzPhen})$ exhibited almost identical emission spectrum in DCM. Therefore, incorporating electron-acceptor substituent group into oxadiazole unit is available for the enhancement of Eu^{3+} emission in europium complexes. In order to further understand the emission property of these bipolar-transporting europium complexes, the emission quantum yields were measured using $\text{EuCl}_3 \cdot 6\text{H}_2\text{O}$ ($\Phi_f = 0.73\%$ in water) as the standard at room temperature based on the literature.²⁶ The measured emission quantum yield values of $\text{Eu}(\text{DBM})_3(\text{Phen})$, $\text{Eu}(\text{DBM})_3(\text{HPhOXD6CzPhen})$, $\text{Eu}(\text{DBM})_3(\text{FPhOXD6CzPhen})$, $\text{Eu}(\text{DBM})_3(\text{MePhOXD6CzPhen})$,

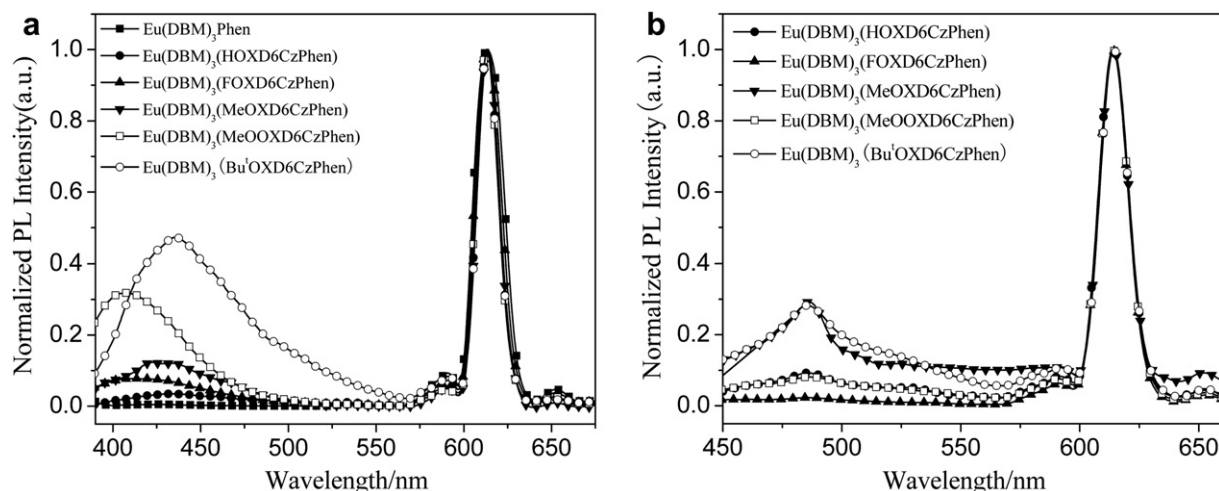


Figure 2. Photoluminescence spectra of europium complexes in CH_2Cl_2 (a) and in their neat (b).

$\text{Eu}(\text{DBM})_3(\text{MeOPhOXD6-CzPhen})$, and $\text{Eu}(\text{DBM})_3(\text{Bu}^t\text{PhOXD6CzPhen})$ were 0.78%, 9.9%, 10.5%, 10.1%, 9.5% and 10.3%, respectively. These values are about 12 fold higher emission quantum yields than that of the $\text{Eu}(\text{DBM})_3\text{Phen}$ complex. Among these bipolar-transporting europium complexes, $\text{Eu}(\text{DBM})_3(\text{FPhOXD6CzPhen})$ presented highest quantum yield. This indicates incorporating a bipolar-transporting unit into ligand of phenanthroline can facilitate the enhancement of emission quantum yield of its europium complex. Especially, attaching a fluorine substituent group with electron acceptor property into the bipolar-transporting unit is more available to improve emission property.

3.5. Electrochemical property

All bipolar-transporting europium complexes presented reversible reduction waves (E_{red}) at -1.53 to -1.94 V versus the saturated calomel electrode (SCE), but their oxidation waves were disappeared. The oxidation potential (E_{ox}) had to be estimated based on energy band gap (E_g) and E_{red} , in which E_g was estimated based on the UV–vis absorption edge. Thus, the highest occupied molecular orbital (HOMO) and the lowest unoccupied molecular orbital (LUMO) energy levels (E_{HOMO} and E_{LUMO}) of europium complexes are calculated according to the empirical relationship formula: $E_{\text{HOMO}} = -e(E_{\text{ox}} + 4.38)$ and $E_{\text{LUMO}} = -e(E_{\text{red}} + 4.38)$, proposed by Brédas group.²⁷ All the electrochemical data of these europium complexes are listed in Table 1. The HOMO and LUMO energy levels of the bipolar-transporting europium complexes are -5.63 eV to -5.91 eV and -2.44 eV to -2.87 eV, respectively. Compared to the $\text{Eu}(\text{DBM})_3\text{Phen}$ complex, these bipolar-transporting complexes exhibited a decrease in the HOMO and LUMO energy levels. The decreased LUMO energy levels are available to facilitate electron injection and transportation from cathode to emitters of europium complexes. Therefore, incorporating both hole-transporting carbazole and electron-transporting oxadiazole unit into ligand can significantly tune electrochemical and carrier-transporting property of its europium complex.

4. Conclusion

In summary, a class of bipolar-transporting europium complexes with both carbazole and oxadiazole units were obtained. These bipolar-transporting europium complexes exhibited higher thermal stability and better optophysical properties than $\text{Eu}(\text{DBM})_3\text{Phen}$. A red sharp emission peaked at 614 nm with a significantly increased emission quantum yield was observed for these

bipolar-transporting europium complexes in DCM solution. The improved optophysical properties are available for this class of europium complexes to become promising red-emitting electroluminescent materials. As for research in electroluminescent properties of these bipolar-transporting europium complexes, we are in progress.

Acknowledgements

This work was supported by the National Natural Science Foundation of China (20772101 and 20872124), the Science Foundation of Hunan Province (2009FJ2002 and 2007FJ3017), Teachers Fund for the Doctoral Program of Higher Education of China (200805301013), the Postgraduate Science Foundation for Innovation in Hunan Province (S2008 yjscx09 and CX2009B124) and the Hunan Undergraduate Innovation Experiment Plan.

Supplementary data

Figure S1. TG curves of europium complexes recorded in dynamic nitrogen atmosphere (50 mL/min) and heating rate of $20^\circ\text{C}/\text{min}$. Supplementary data associated with article can be found in online version at doi:10.1016/j.tet.2010.07.003.

References and notes

- Hong, Z.; Liang, C.; Li, R.; Li, W.; Zhao, D.; Hong, L. S.; Lee, S. T. *Adv. Mater.* **2001**, *13*, 1241.
- Liang, Q. D.; Cai, Q. J.; Neoh, K. G.; Zhu, F. R.; Huang, W. J. *Mater. Chem.* **2004**, *4*, 2741.
- Robinson, M. R.; O'Regan, M. R.; Bazan, G. C. *Chem. Commun.* **2000**, 1645.
- Liang, F.; Zhou, Q.; Cheng, X.; Wang, L.; Jiang, X.; Wang, F. *Chem. Mater.* **2003**, *15*, 1935.
- Pei, J.; Liu, X.; Yu, W.; Lai, Y.; Liu, Y.; Cao, Y. *Macromolecules* **2002**, *35*, 7274.
- O'Riordan, A.; O'Connor, E.; Moynihan, S.; Llinares, X.; Deun, R. V.; Fias, P.; Nockemann, P.; Binnemans, K.; Redmond, G. *Thin Solid Films* **2005**, *491*, 264.
- Canzler, T. W.; Kido, J. *Org. Electron.* **2006**, *7*, 29.
- Liu, Y.; Li, J. D.; Li, C.; Song, J. G.; Zhang, Y. L.; Peng, J. B.; Wang, X. Y.; Zhu, M. X.; Cao, Y.; Zhu, W. G. *Chem. Phys. Lett.* **2007**, *433*, 331.
- McGehee, M. D.; Bergstedt, T.; Zhang, C.; Saab, A. P.; O'Regan, M. B.; Bazan, G. C.; Srdanov, V. I.; Heeger, A. J. *Adv. Mater.* **1999**, *11*, 1349.
- Guan, M.; Bian, Z. Q.; Li, F. Y.; Xin, H.; Huang, C. H. *New J. Chem.* **2003**, *27*, 1731.
- Xin, H.; Li, F. Y.; Guan, M.; Huang, C. H.; Sun, M.; Wang, K. Z.; Zhang, Y. A.; Jin, L. P. *J. Appl. Phys.* **2003**, *94*, 4729.
- Li, S. F.; Zhong, G. Y.; Zhu, W. H.; Li, F. Y.; Pan, J. F.; Huang, W.; Tian, H. *J. Mater. Chem.* **2005**, *15*, 3221.
- Li, S. F.; Zhu, W. H.; Xu, Z. Y.; Pan, J. F.; Tian, H. *Tetrahedron* **2006**, *62*, 5035.
- Zhu, Z. W.; Liu, Y.; Luo, C. P.; Hu, Z. Y.; Zhu, M. X. *ZhongGuo FaMing ZhuanLi ZL*, 2006-100325507.
- Liang, F. S.; Zhou, Q. G.; Cheng, Y. X.; Wang, L. X.; Ma, D. G.; Jing, X. B.; Wang, F. S. *Chem. Mater.* **2003**, *15*, 1935.
- Liu, Z.; Wen, F. S.; Li, W. L. *Thin Solid Films* **2005**, *478*, 265.

17. Tang, H. J.; Tang, H.; Zhang, Z. G.; Cong, C. J.; Zhang, K. L. *Synth. Met.* **2009**, *159*, 72.
18. Lin, S. L.; Chan, L. H.; Lee, R. H.; Yen, M. Y.; Kuo, W. J.; Chen, C. T.; Jeng, R. J. *Adv. Mater.* **2008**, *20*, 3947.
19. Liu, Y.; Su, G. J.; Xing, K. Q.; Gan, Q.; Yang, Y. P.; Wang, X. Y.; Zhu, W. G. *Nat. Sci. J. Xiangtan Univ.* **2006**, *28*, 68 (in Chinese).
20. Xu, Z. W.; Li, Y.; Ma, X. M.; Gao, X. D.; Tian, H. *Tetrahedron* **2008**, *64*, 1860.
21. Lecomte, J. P.; Mesmaeker, A. K. D.; Lhomme, J. J. *Chem. Soc., Faraday Trans.* **1993**, *89*, 3261.
22. Ueno, K.; Martell, A. E. *J. Phys. Chem.* **1956**, *60*, 1270.
23. Bünzli, J. C. G.; Moret, E.; Foiret, V.; Schenk, K. J.; Mingzhao, W.; Linpei, J. *J. Alloys Compd.* **1994**, *107*, 207.
24. Braga, S. S.; Ferreira, R. S.; Goncalves, I. S.; Pillinger, M.; Carlos, L. D. J. *Phys. Chem. B* **2004**, *106*, 11430.
25. de Sa, G. F.; Malta, O. L.; de Mello Donega, C.; Simas, A. M.; Longo, R. L.; Santa-Cruz, P. A.; da Silva, E. F. J. *Coord. Chem. Rev.* **2000**, *196*, 165.
26. Bian, Z. Q.; Gao, D. Q.; Guang, M.; Xin, H.; Li, F. Y.; Wang, K. Z.; Jin, L. P.; Wang, C. H. *Sci. in China. B. Chem.* **2004**, *34*, 113 (in Chinese).
27. Brédas, J. L.; Silbey, R.; Boudreaux, D. S.; Chance, R. R. *J. Am. Chem. Soc.* **1983**, *105*, 6555.